

Modelling of pre-eruptive magnetic structure: the need to get the electric currents right!



Laboratoire de Physique des Plasmas

RoCMI – Svalbard – March 2nd 2023

Étienne Pariat¹, G. Valori², S. Masson^{1,3}

¹ Laboratoire de Physique des Plasmas, Sorbonne Université, École polytechnique, Institut Polytechnique de Paris, Université Paris Saclay, Observatoire de Paris-PSL, CNRS, Paris, France

² Max-Planck-Institut für Sonnensystemforschung, Justus-von-Liebig-Weg 3, Göttingen, Germany

³ Station de Radioastronomie de Nançay, Observatoire de Paris, CNRS, PSL, Université d'Orléans, Nançay, France

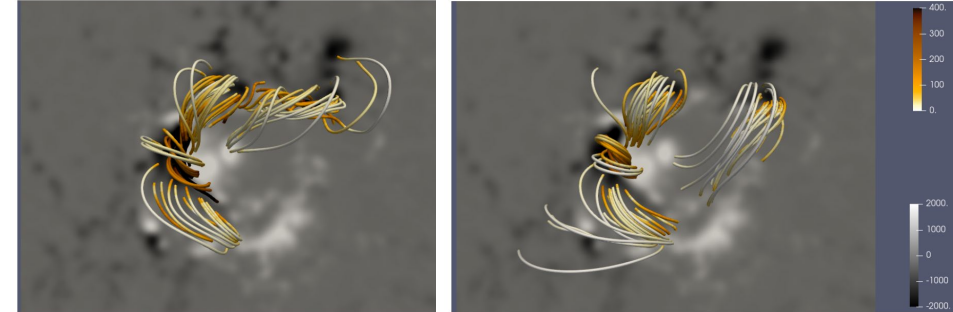


Introduction : Trigger of eruption enigma



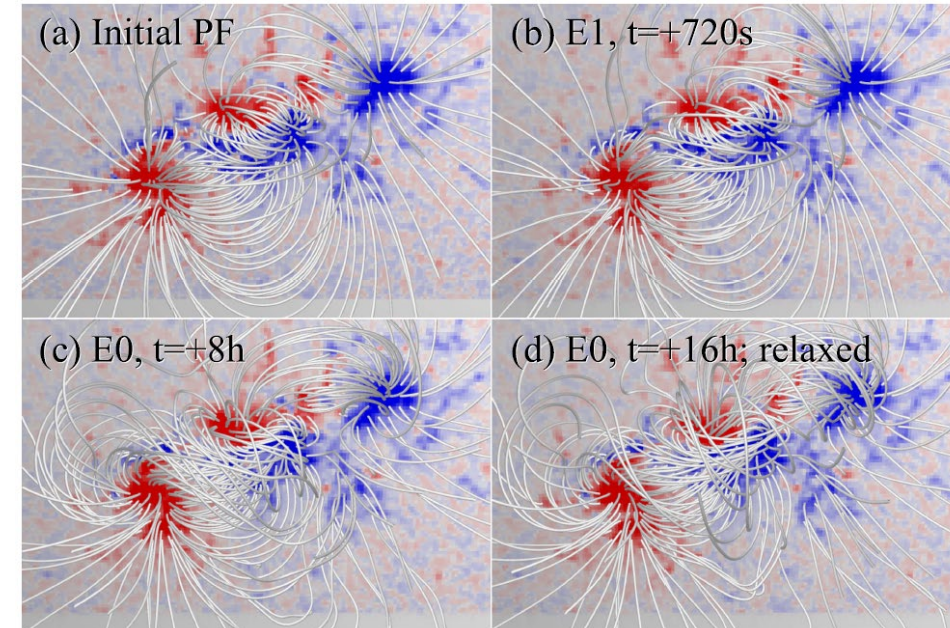
- Trigger of eruptions remains a major unresolved problem :
 - No consensus on the generation mechanism of solar eruptions
 - Large scale (MHD) instability: e.g. kink / torus
 - Instability in electric current sheet @ reconnection site
- Stem from the lack of proper knowledge of the exact pre-eruptive state of the magnetic system
 - Observation provides limited information : almost only photo. **B**
 - Numerical model idealized & limited by observational input
- **How are 3D coronal field of eruptive systems modeled?**
 - **(Quasi-) Static models: coronal B extrapolations**
 - Model the pre-eruptive system from observational dataset as close as possible from eruption onset
 - **Dynamic models: data driven/inspired simulations**
 - Numerically evolve toward eruption, using consistent boundary forcing, a model obtained from an early, hopefully more simple, stage of the eruptive system.

(Moraitis et al. 19)



Same obs. input, different reasonable reconstruction parameters

(Hayashi et al. 18)



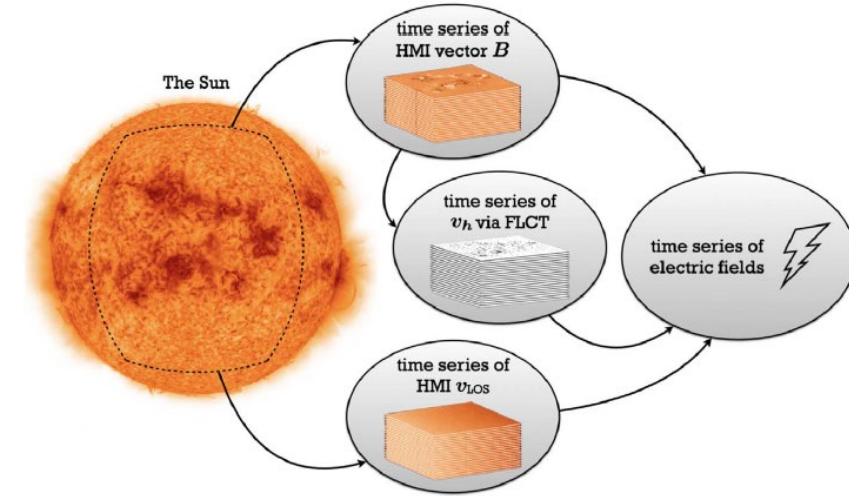
Importance of electric fields / currents



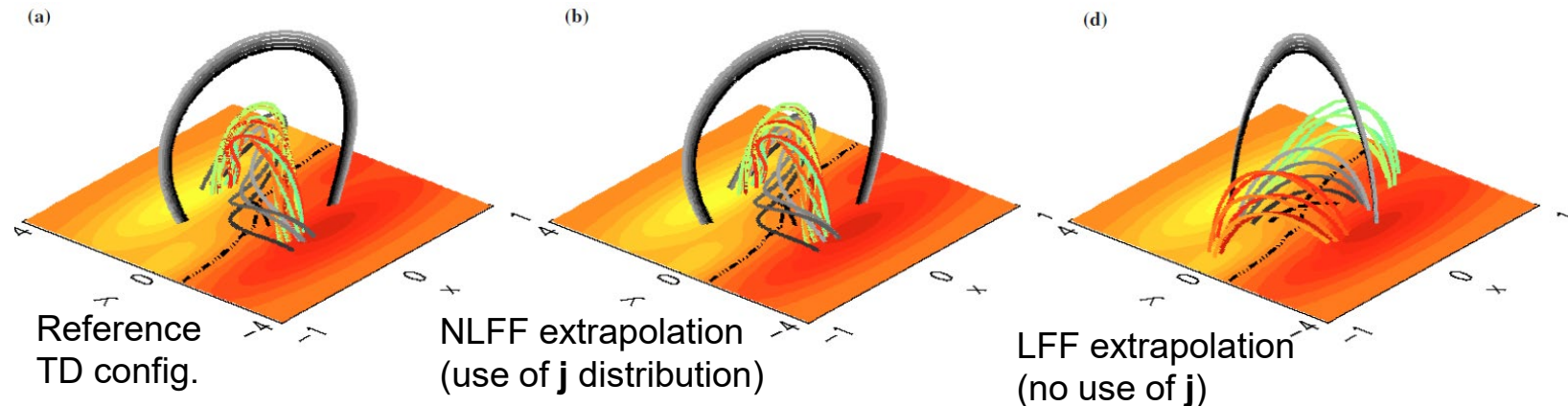
- In both approaches, to properly represent the complexity of the coronal field, it is essential to use the full photospheric vector B field

→ electric field (E) & electric currents (j)

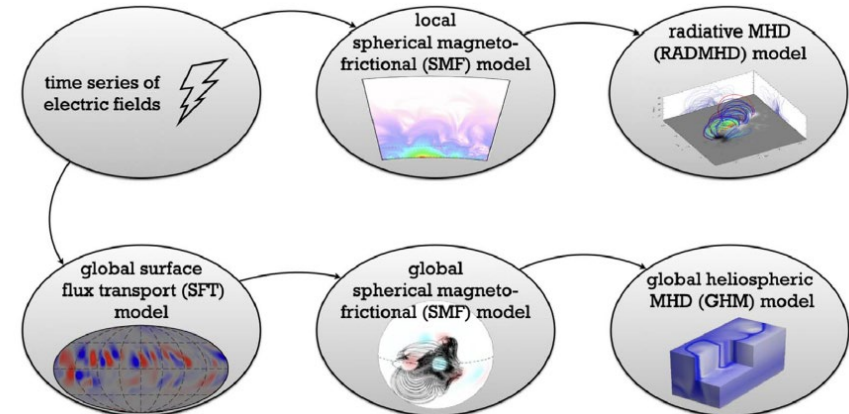
- NLFF vs potential/LFF extrapolations (e.g. Valori et al. 10)
- Simulations data-driven thanks to electric field : e.g. GCEM model (Hoeksama et al. 20) ; TMF simulation (Lumme et al. 22) using "PDFI" method (Kazachenko et al. 14; Fisher et al. 20)



(Hoeksama et al. 20)



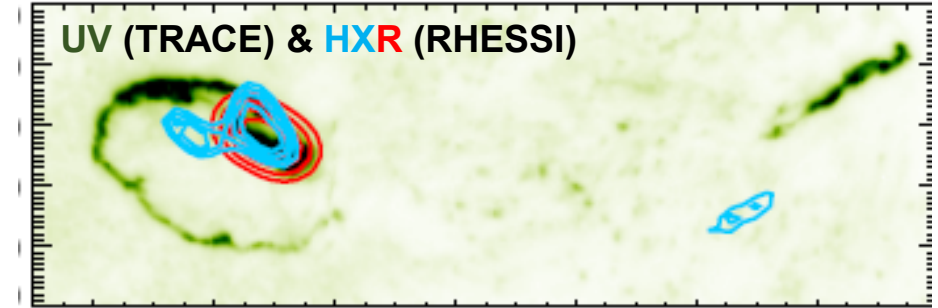
(Valori et al. 10)



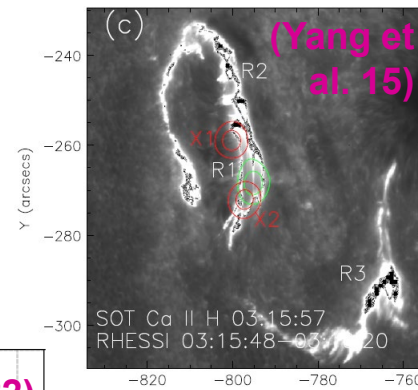
Modelling of circular ribbon flares



- Circular ribbons flares are a subgroup of flaring events (Ugarte-Urra et al. 2007, Masson et al. 09,17, Reid et al. 12, Deng et al. 13, Yang et al. 2015, Janvier et al. 16, Mitra 21, ...)
 - 3 ribbons are observed at \sim the same time
 - 1 main circular ribbon ;
 - 1 ribbon within the circular one;
 - 1 ribbon outside further away
- Statistical analysis of 134 circular ribbon flares (Zhang et al. 22)



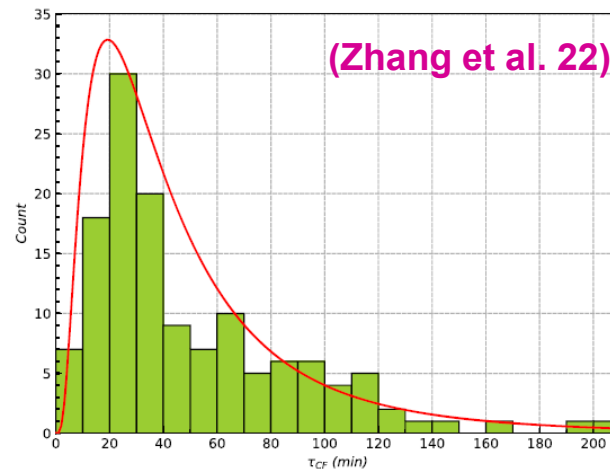
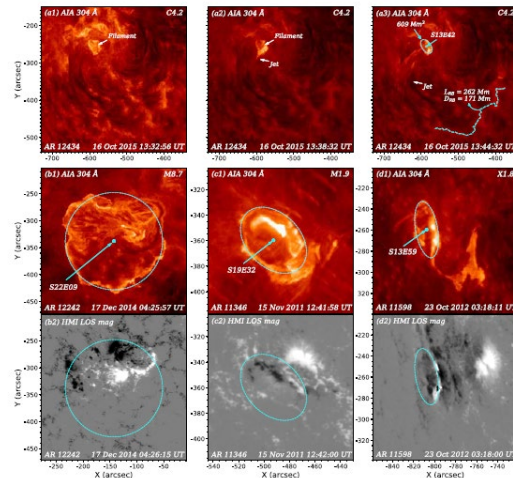
(Reid et al. 12)



(Yang et al. 15)



(Deng et al. 13)



(Zhang et al. 22)

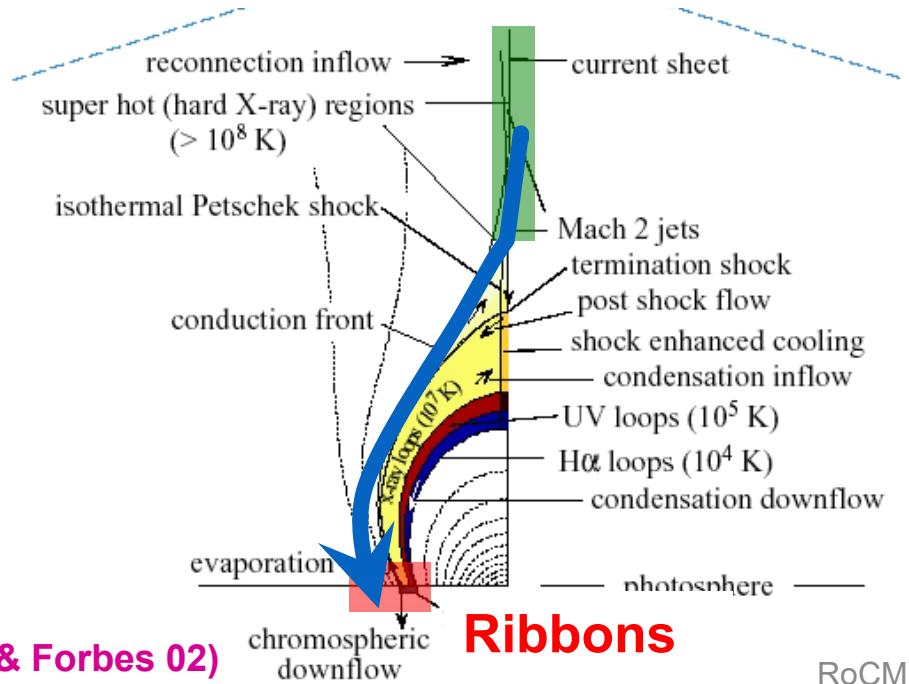
Table 3
Numbers of CFs Associated with RBs, Type III Radio Bursts, Jets, Minifilament Eruptions, and CMEs

Activity	B-class	C-class	M-class	X-class	Total
CF	4	82	40	8	134
RB	1	40	28	7	76
type III	0	36	24	3	63
jet	1	43	21	4	69
FE	1	25	18	7	51
CME	0	17	14	6	37

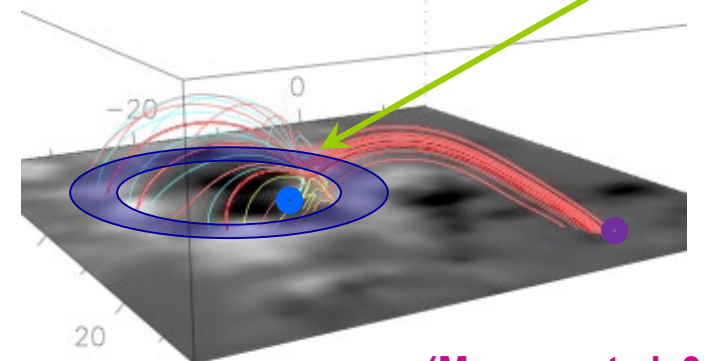
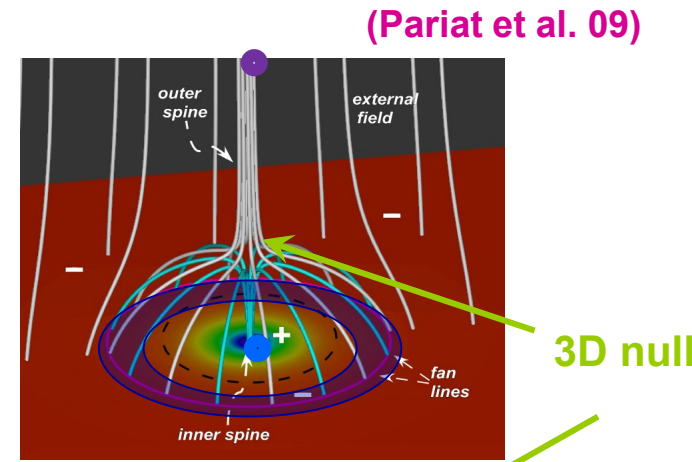
Topology and ribbons : the 3D null case



- Standard model: **accelerated particles/energy** flowing from the **reconnection site**. Interaction with lower denser layers → **Ribbons** formation
- **3D null points** are preferential sites for current build-up & **reconnection**
 - → **Ribbons** are located at the footpoint of the (**quasi-**) **separatrices** originating from the **3D null point**
- → **Theoretical distribution of 3D null points ribbons:**
1 circular ribbon + 1 inner ribbon inside + 1 outer ribbon



(Lin & Forbes 02)



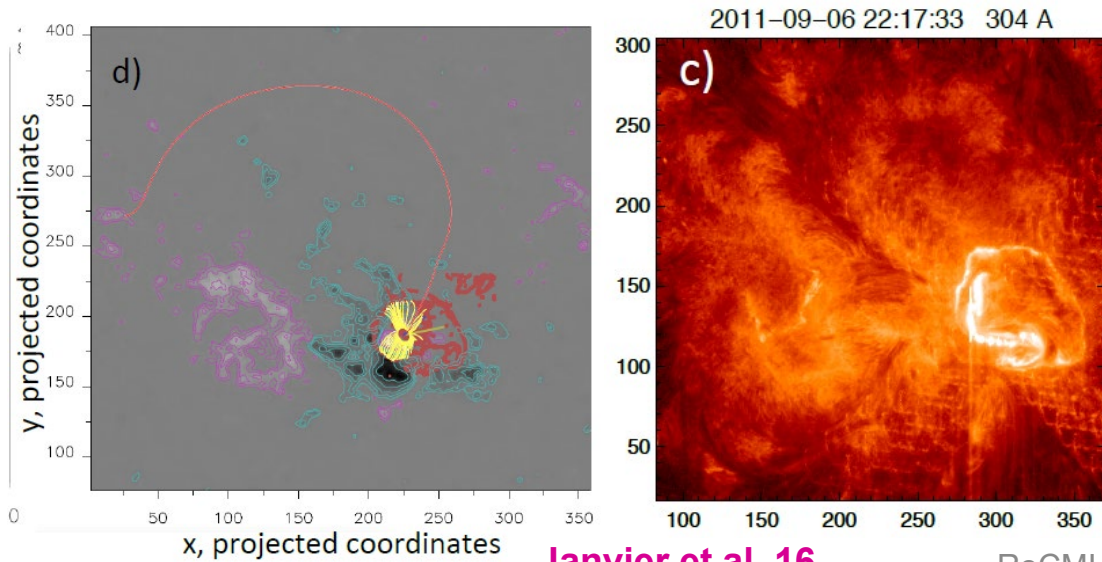
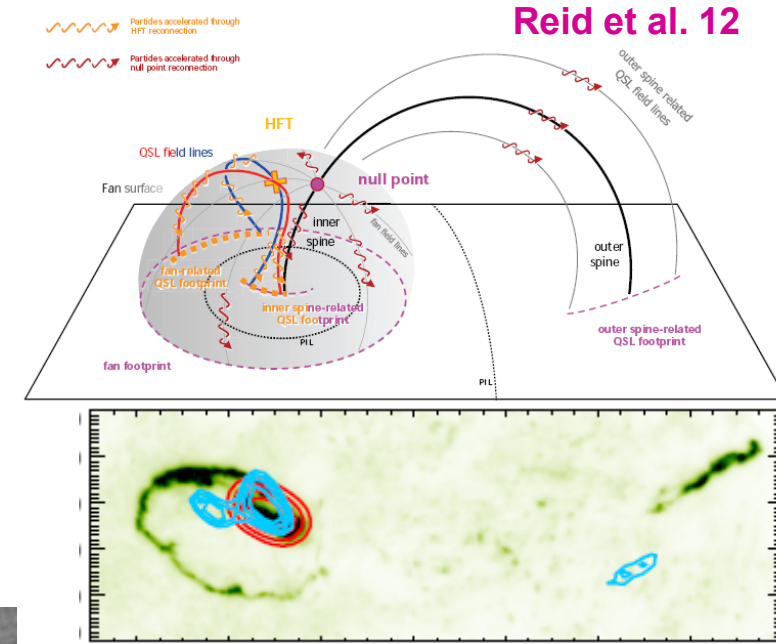
(Masson et al. 09)

- **3D null point:** magnetic singularity (**B=0**)
- **Separatrices** (connectivity interface) of a **3D null point:**
 - **1 dome-like fan** separatrix surface
 + **1 inner spine** & **1 outer spine** separatrices

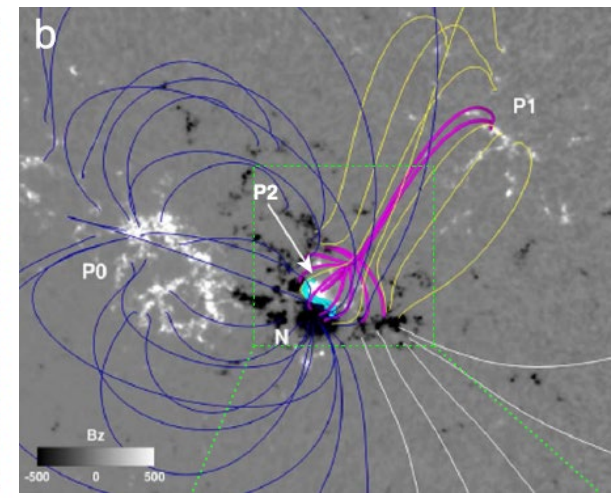
Circular ribbon flare \Leftrightarrow 3D null topology



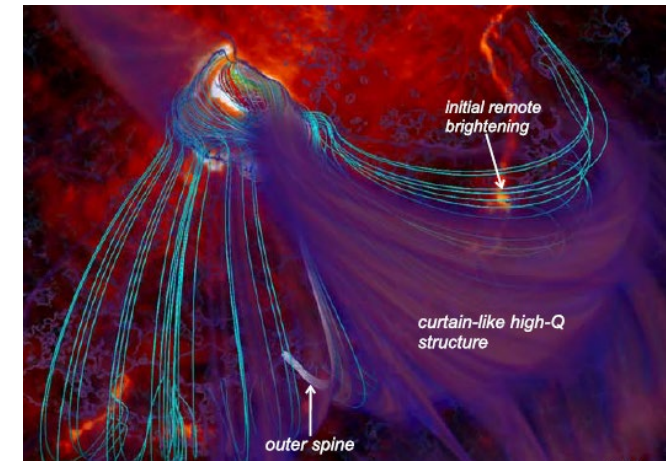
- **Circular ribbons flares are indeed associated with 3D coronal null point topologies** (e.g. Masson et al. 09, 17, Wang & Liu 12, Deng et al. 13, Janvier et al. 16, Jiang et al. 18, Nayak et al; 19, Liu et al. 20, Prasad et al. 20, Kumar et al. 22, ...)
- Circular ribbons match well the footprint position of the fan
- **However, positions of outer ribbons are frequently not well recovered by magnetic field models**
- Locations of ribbons are usually several tens of Mm from the predictions of the B field models



Janvier et al. 16



Jiang et al. 18

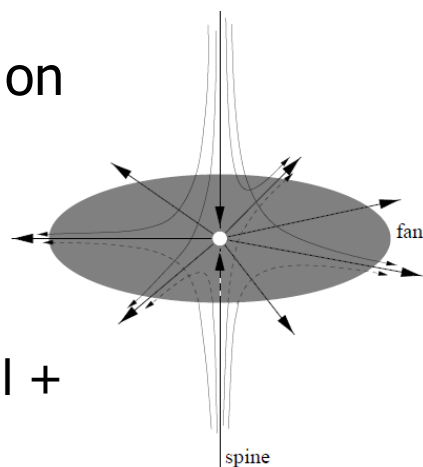


Liu et al. 20

Electric currents (\mathbf{j}) at a 3D null

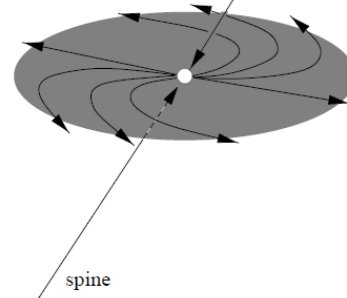


- The shape & structure of a 3D null depend on the distribution of the electric currents
 - Fan position** strongly constrained by photospheric \mathbf{B} distribution
 - Null B flux under fan dome
 - Spine position** constrained by \mathbf{j} at the null + large scale \mathbf{B}
- Position of spine is a strong test of the quality of the 3D B field coronal model**



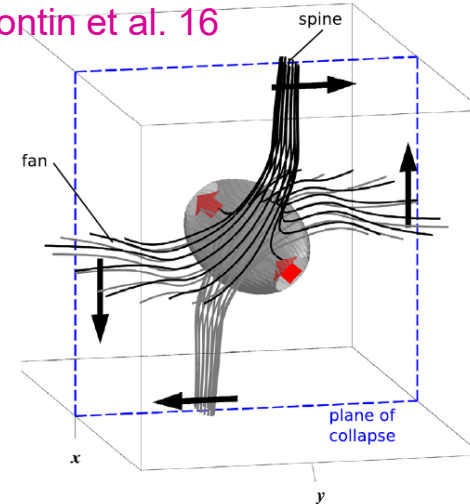
Potential 3D null point ($\mathbf{j}=0$)

Longcope et al. 05

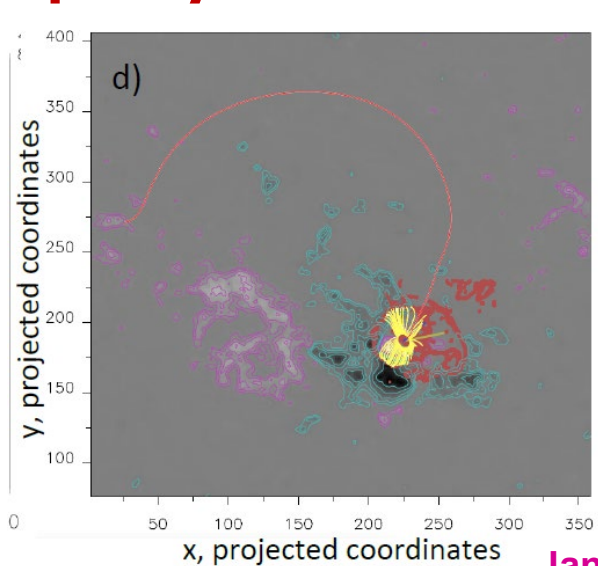


3D null point with $\mathbf{j} \neq 0$

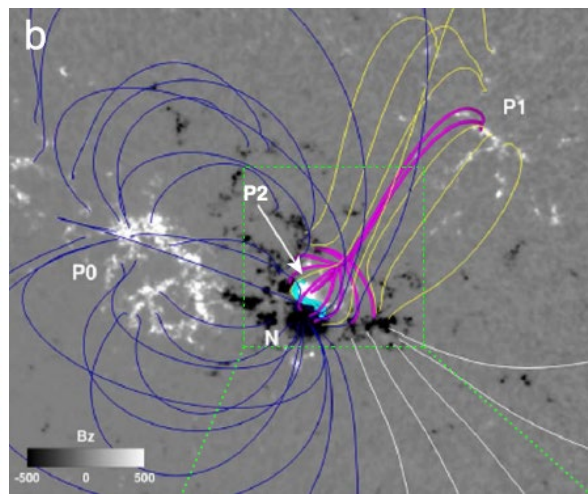
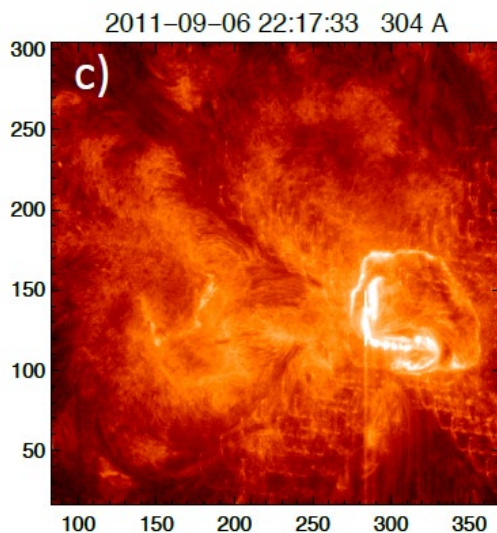
Pontin et al. 16



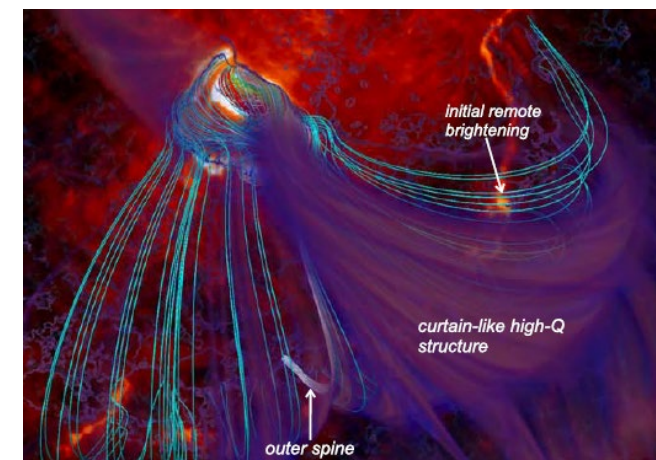
Generic shape of reconnecting 3D null



Janvier et al. 16



Jiang et al. 18

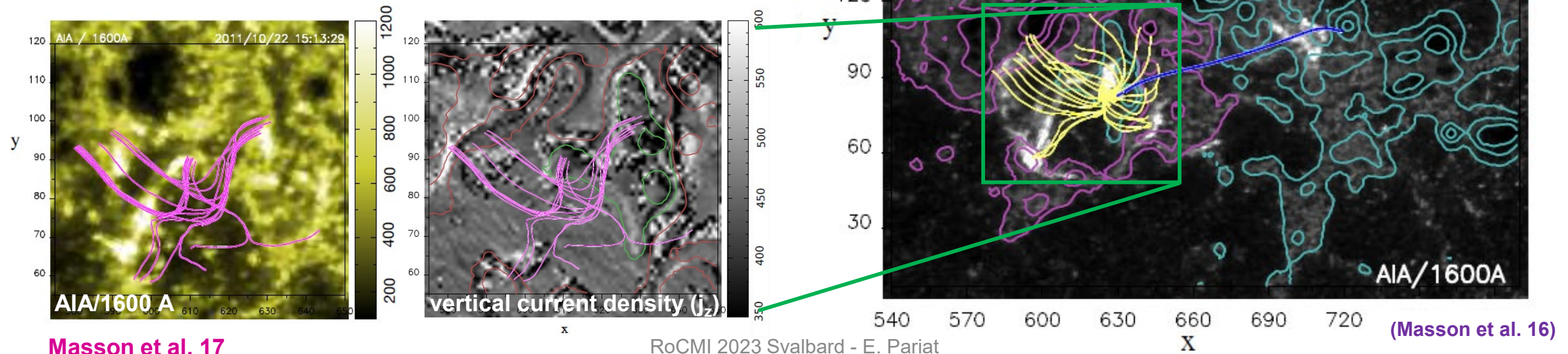


Liu et al. 20

Example of a well reconstructed circular ribbon flare



- **Masson et al. 17**: 3D model of a compact circular ribbon flare (SOL2011-10-22-1521)
- Strong care of the proper inclusion of the electric current (j_z) in the NLFFF extrapolation
- 3D non-linear force free (NLFF) extrapolation with the magneto-frictional method of **Valori et al. 10**
 - While aiming for FF solution, method is flexible for keeping residual currents in localized regions, e.g. at 3D null point
- **→ 3D model matches the position of the spine ribbons within a few Mms**
 - Enable to study the eruption dynamics with a high degree of confidence: existence of flux rope under fan dome, dynamics of late EUV phase,

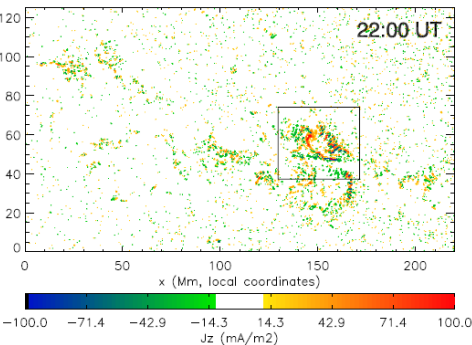
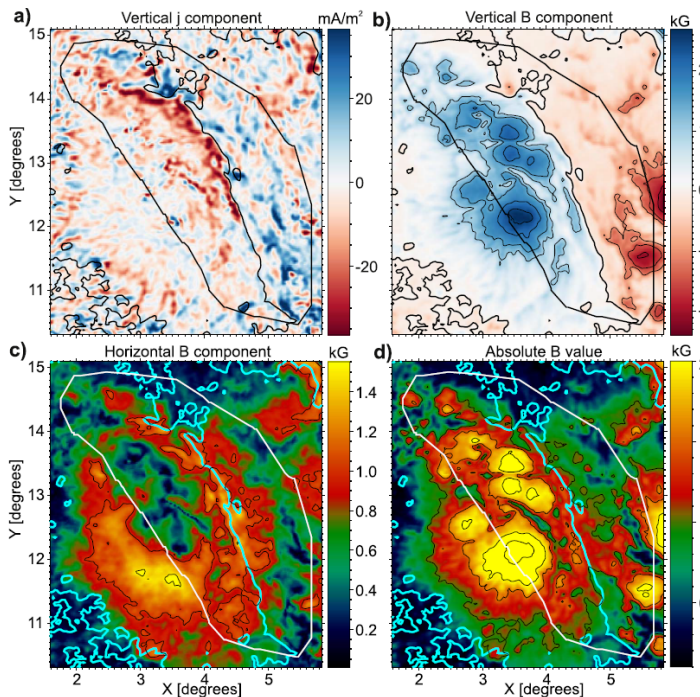
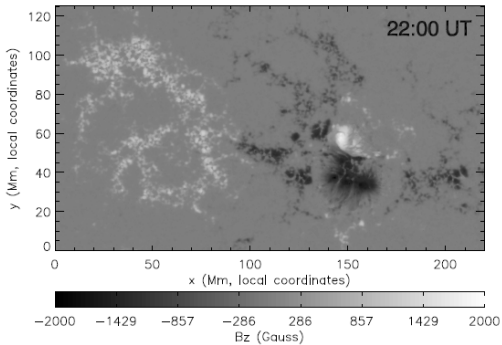


Electric current measurements and the 180° ambiguity issue



- Estimations and study of vertical electric current density (j_z) is becoming a standard by-product of vector magnetic field measurements (e.g. Janvier et al. 16; Barczynski et al. 20, Artemyev et al. 21)
- Limitation: fundamental 180° ambiguity on measurement of the transverse (to l-o-s) \mathbf{B} component
 - Oppositely directed transverse fields (by 180°) produce the very same Zeeman signal

$$\mathbf{B}_{\text{obs}} = B_{\text{los}} \mathbf{e}_{\text{los}} + \zeta B_{\text{tr}} \mathbf{e}_{\text{tr}} \quad \text{with ambiguity } \zeta = \pm 1$$



- **Estimation of j_z strongly dependent on 180° fundamental ambiguity**

$$j_z = \zeta \left(\frac{\partial B_y}{\partial x} - \frac{\partial B_x}{\partial y} \right)$$

- Removal of the 180° ambiguity is usually done thanks to empirical method (model dependent):
 - cf. reviews of Metcalf et al. 06, Leka et al. 09
 - Less-energetic/ “well-behaved” ambiguity solution usually preferred ; possibly in contradiction to pre-eruptive state

Janvier et al. 16

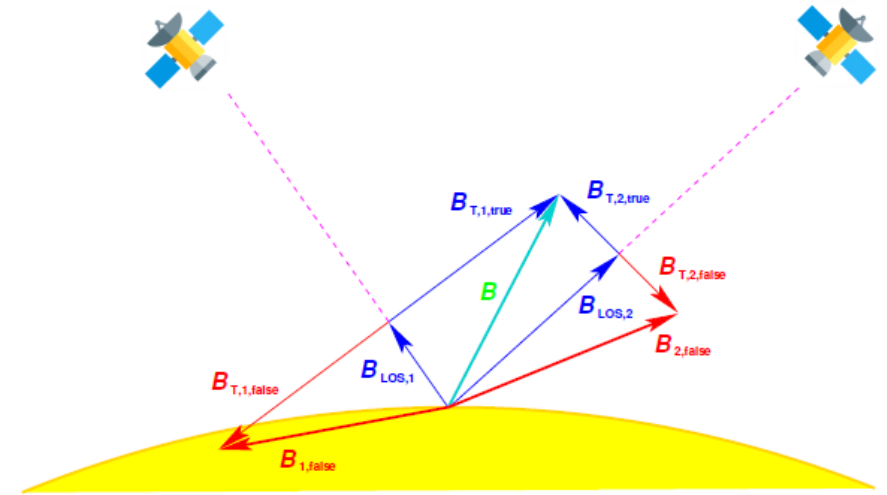
Artemyev et al. 21

Stereoscopic Disambiguation Method (SDM)



Rouillard et al. 20

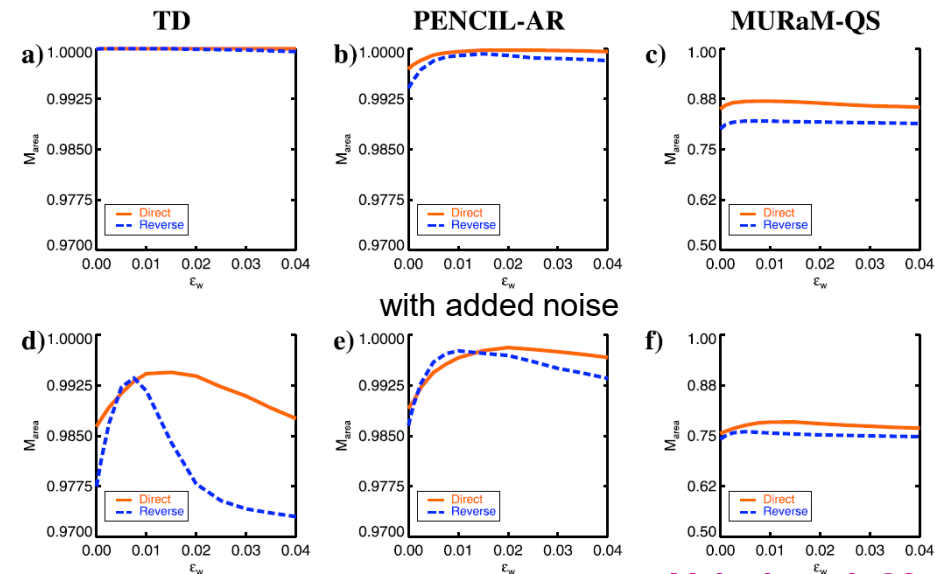
- For the first time, Solar Orbiter's PHI instrument (Solanki et al. 20) is providing \mathbf{B} measurements away of the Sun-Earth line.
- **Observations of the same solar region from both PHI and Earth's orbit (e.g. SDO/HMI) can enable the unique observational removal of the 180° ambiguity.**
 - Line of sight measurement of one of the spacecraft shall enables the unambiguous choice on the direction of the transverse field of the second spacecraft.
 - Application to real data may be hardous: instruments do not look at the same plasma column along line-of-sight.



- **Stereoscopic Disambiguation Method (Valori et al. 22)**

$$\mathbf{B}_{\text{obs}} = B_{\text{los}} \mathbf{e}_{\text{los}} + \zeta B_{\text{tr}} \mathbf{e}_{\text{tr}} \quad \zeta = \frac{B_{\text{los}}^{\text{B}} - B_{\text{los}}^{\text{A}} \cos \gamma}{B_{\text{w}}^{\text{A}} \sin \gamma}$$

- Proof-of-concept and rigorous test on diverse synthetic dataset (analytical field, MHD sim. of AR; radiative transfer in quiet sun)
- High accuracy of the method

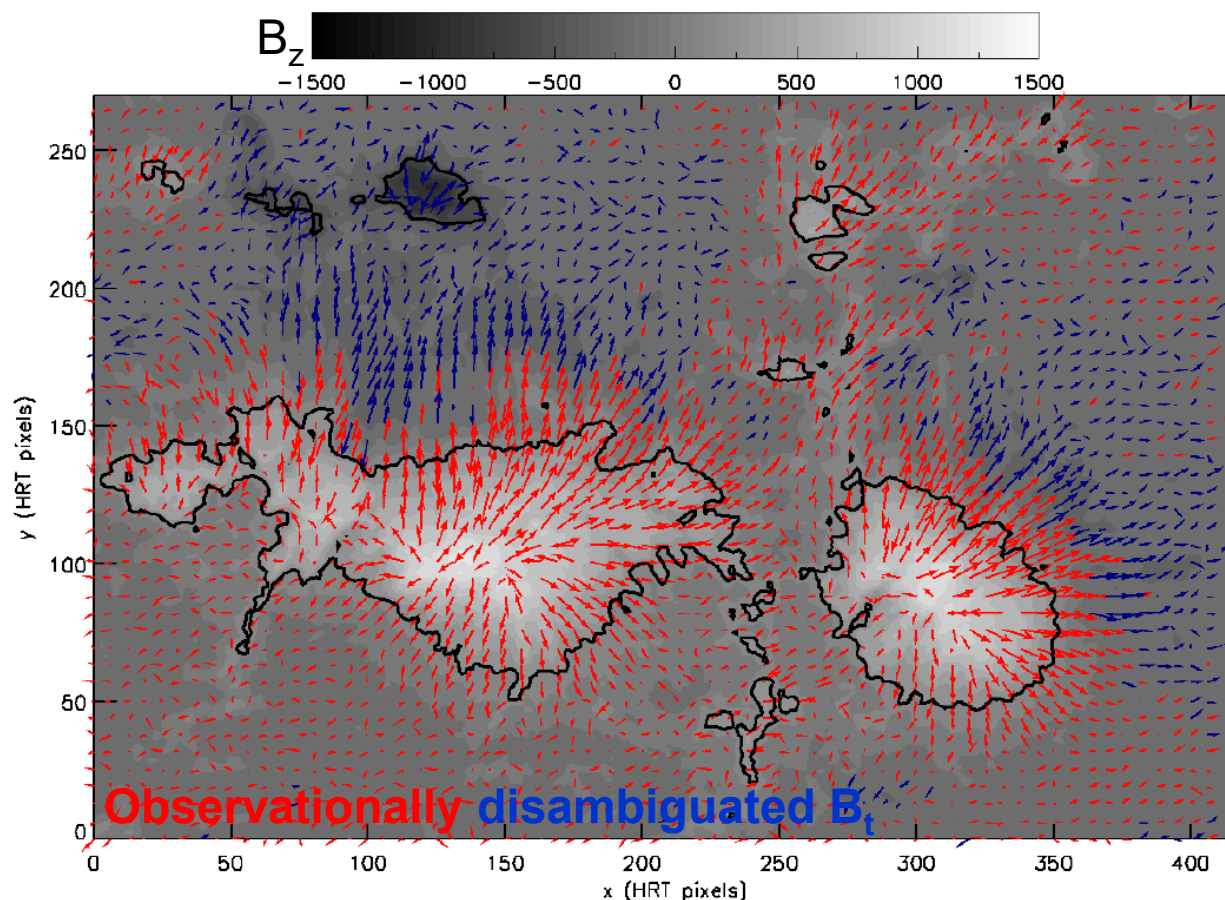
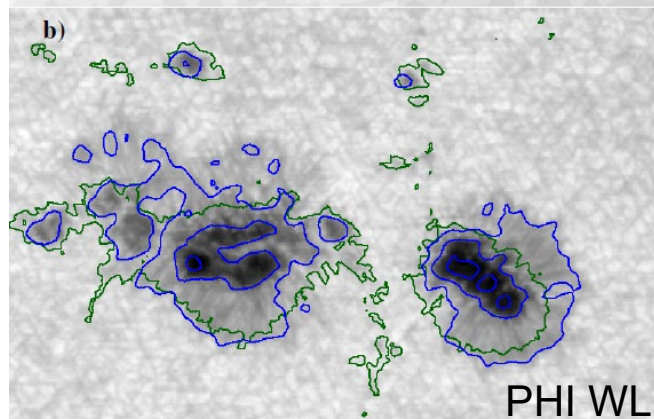
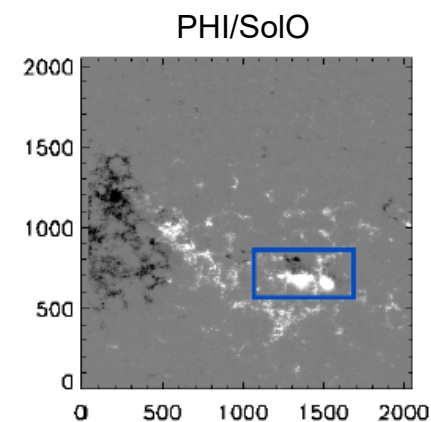
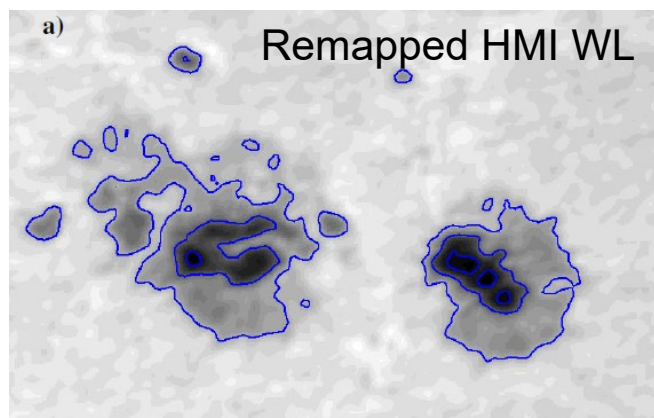
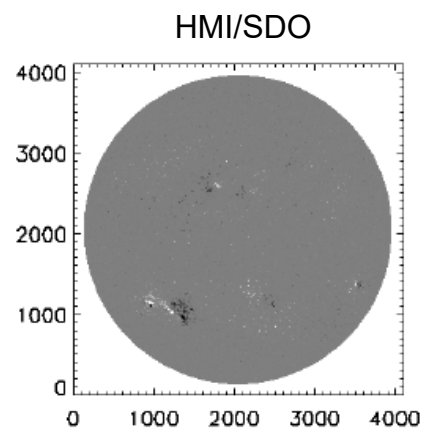


Valori et al. 22

First observationally disambiguated vector magnetogram



- Application of the SDM method to observed data from HMI/SDO and PHI/SolO
 - March 17th 2022, ~3:45 ; separation angle of 27°
- **Successful observational disambiguation of the 180° ambiguity (Valori et al. in revision)**



Summary



- Electric current density/electric field is a key element for the proper modeling of the coronal magnetic field.
- **Models in which electric currents are carefully inputted are able to reproduce & explain well multiple eruptive features**
 - e.g. circular ribbon flare model of **Masson et al. 17**
- SoI/O/PHI now enables the observational removal of 180° ambiguity
→ **First observationally disambiguated vector magnetogram (Valori et al. in rev) thanks to the Stereoscopic Disambiguation Method (Valori et al. 22)**
- Open new possibilities
 - observationally benchmark single-view measurement of current density obtain from usual 180° ambiguity resolution method
 - new generation of coronal field models

